Materials Research Proceedings **26** (2023) 3-8 https://doi.org/10.21741/9781644902431-1

A novel one domain approach for free fluid-porous medium transport simulation - preliminary results

Costanza Aricò[1,2,a *], Martin Schneider[2,b], Tullio Tucciarelli[1,c] and Rainer Helmig[2,d]

[1]Department of Engineering, University of Palermo, Viale delle Scienze, 90128, Palermo, Italy

[2]Institute for Modelling Hydraulic and Environmental Systems, University of Stuttgart, Pfaffenwaldring 61, 70569 Stuttgart, Germany

[a]costanza.arico@unipa.it, [b]martin.schneider@iws.uni-stuttgart.de, [c]tullio.tucciarelli@unipa.it, [d]rainer.helmig@iws.uni-stuttgart.de

Keywords: Free Flow, Porous Medium, Transport Phenomena, Numerical Solver

Abstract. We present a new numerical solver for free-fluid flowing over and inside a porous medium. It is based over a macroscopic approach and one fictitious medium is assumed inside the domain, according to the One Domain Approach. Preliminary results are shown and compared with the ones provided by the well-known DuMux solver which applies a two Domain Approach.

Introduction

Transport phenomena of combined free fluid (ff) and porous medium (pm) flow occur in several industrial, environmental and biological applications (e.g., surface and groundwater flow, contaminant transport from lakes by groundwater, fuel cells, oil filters, blood flow in vessels and tissue, transfer of therapeutic agents).

The related mass, momentum and energy transport mechanisms at the ff–pm interface have been intensively investigated during the last decades applying two main approaches, the formulations at the micro- and macro-levels, respectively.

At the microscopical level, the porous medium is assumed as a connected domain of pore spaces filled with the fluid. The flow is governed by Navier–Stokes (or Stokes) equations, and no–slip boundary conditions are imposed on the interfaces between fluid and solid particles of the porous medium. The main drawback of this approach is its application for real problems, due to the huge amount of CPU time and computer memory storage, as well as the lack of an exact knowledge of the real porous geometry.

At the macroscopical level, the sets of the governing equations are obtained by averaging or upscaling the equations at the microscopic level over a Representative Elementary Volume (REV) [1]. The REV size is much larger than the characteristic size of the pore, but much smaller than the representative size of the domain. Two general different approaches have been derived at the macroscale, namely the Two-Domain Approach (TDA) and the One-Domain Approach (ODA) [1].

In TDA, the domain is split into two regions, and, in the most general case, the Navier–Stokes equations describe the fluid flow in the ff domain, while the Darcy's law is applied in the pm region. This is the most difficult approach from a mathematical point of view, since the two sets of governing equations are completely different systems of Partially Differential Equations (PDEs) and need interface conditions (IFCs). A sharp interface is assumed, where appropriate boundary conditions are imposed (typically, the conservation of mass, the balance of normal forces and the Beavers–Joseph condition (BJC) for the tangential velocity components [2]).

On the contrary, in ODA, the porous layer is regarded as a pseudo-fluid and the composite region free fluid-porous medium is treated as a continuum. One set of PDEs is assumed, typically the Brinkman or the (Navier)-Stokes-Brinkman equations (e.g., [1, 3]). The transition from the

fluid to the porous medium is achieved through a continuous spatial variation of physical properties, such as permeability and porosity inside a transition layer (TL) which separates the homogeneous ff region from the bulk porous medium. The major drawback of the ODA is related to the knowledge of the size of the TL between the two homogeneous regions and how the physical parameters of the porous medium change inside it.

In the recent literature, some ODA have been proposed for the Brinkman equations [4] or a momentum equation having a Darcy form, including inertial and slip effects [5].

In the present paper, we present a novel numerical solver for ODA for incompressible and single-phase fluid over a saturated anisotropic porous medium. The governing equations, derived by averaging the pore scale microscopic Navier-Stokes equations, are the Incompressible Navier-Stokes-Brinkman equations (INSBEs), discretized over general unstructured meshes.

Preliminary model results are shown.

The Governing Equations and spatial discretization

The governing equations are a set of Partial Differential Equations (PDEs), the INSBEs,

$$\nabla \cdot \boldsymbol{u} = 0 \tag{1},$$

$$\frac{\partial \boldsymbol{u}}{\partial t} + \boldsymbol{u} \cdot \nabla \boldsymbol{u} + \nabla \Psi - \upsilon \Delta_2 \boldsymbol{u} + \frac{\upsilon \varepsilon}{\boldsymbol{K}} \boldsymbol{u} = 0 \tag{2},$$

where t is the time, $\mathbf{u}$ is the fluid velocity vector (with u and v its x and y components), υ is the kinematic viscosity of the fluid, Ψ is the kinematic pressure of the fluid ($\Psi = p/\rho$ with p and ρ the fluid pressure and fluid constant density, respectively), $\mathbf{K}$ the permeability matrix of the porous medium, symmetric and positive-definite, and ε is the porosity of the porous medium. The last term on the l.h.s. of Eq. (2) takes into account the drag effects due to interaction of the fluid with the solid particles of the porous medium. The set of the governing equations has been derived from the Navier-Stokes equations at the pore-scale, applying average techniques [3, 6]

The computational domain Ω is discretized by means of unstructured triangulations of N_T non-overlapping triangles and N nodes. Inside each triangle e we assume the velocity vector be piecewise constant and $\boldsymbol{u}_e(\boldsymbol{x}) \in \mathbf{X}_e$, where $\mathbf{X}_e$ is the lowest-order Raviart-Thomas (RT-0) space. Ψ is assumed to be piecewise linear inside each triangle. The computational mesh satisfies the Delaunay Property.

In the present algorithm, INSBEs are solved by sequentially applying a fractional time step procedure, by solving consecutively a prediction and two correction steps. The prediction step is solved by applying the MAST (Marching in Space and Time) procedure, recently proposed for the solution of shallow waters, groundwater and incompressible Navier Stokes problems ([7] and cited works). MAST presents some important advantages: 1) explicit handling of the non-linear momentum terms due to a sequential solution of a small Ordinary Differential Equations (ODEs) system for each computational cell, 2) a computational effort proportional to the number of triangular elements and 3) numerical stability with respect to Courant-Friedrichs-Lewy (CFL) numbers also greater than one. The correction steps are solved by a Mixed Hybrid Finite Elements discretization that assumes a Generalized Delaunay mesh condition. They involve the solution of large linear systems, whose matrices are sparse, symmetric, positive definite and diagonally dominant, allowing a well performing condition number and a very fast solution of the associated systems. Strong reduction of the computational effort, in comparison with other numerical schemes (e.g., Lagrangian schemes), is due to the matrix coefficients, which are constant in time and are calculated only once, before the beginning of the numerical iteration loop. Flux continuity at each triangle side is guaranteed, as well as the local and global mass balance (more details in

Materials Research Proceedings **26** (2023) 3-8 https://doi.org/10.21741/9781644902431-1

the cited works). There is no need to compute pressure at each time iteration, but only at target simulation times.

Model Results

1. Comparison with analytical solution and study of convergence order

We assume a 1D domain (see figure 1), with an isotropic porous medium and an analytical velocity profile given by Eqs. (3), continuous from the ff to the pm region.

$$u = 4U_M\left(\left(\frac{y-H}{y_{max}-H}-1\right)\left(\frac{y-H}{y_{max}-H}+\delta\right)\right) \text{ in ff, } u = 4U_M\left(\frac{\varepsilon(2\varepsilon^2-1)e^{\left(\frac{y-H}{\varepsilon(y_{max}-H)}-1\right)}}{1+\varepsilon}-\delta\right) \text{ in pm } (3),$$

with $U_M = \frac{\nabla_x\Psi}{8\nu}(y_{max}-H)^2$, $\nabla_x\Psi$= 1d-08 m/s^2, $\nabla_y\Psi$= 0, $\varepsilon = \varepsilon\left(\sqrt{\frac{k_0}{\nu}}\Big/H\right)$, δ = δ(ε), and k_0 the value of the permeability in the bulk porous medium. Vertical velocity component is zero. A source term vector is computed according to the expression of the velocity and the pressure gradient, in order to set to zero the momentum equation (2). We assume a hyperbolic variation of the permeability and porosity inside the TL, as in Eq. (4),

$$k(\mathbf{x}) = \frac{1}{2}\left((1-k_0)tanh(dist)+(1-k_0)\right) \quad \varepsilon(\mathbf{x}) = \frac{1}{2}\left((1-\varepsilon_0)tanh(dist)+(1-\varepsilon_0)\right) (4),$$

where the distance *dist* from the midline of the TL is shown in Fig. 1 and k_0 = 1d-06 m^2. Two studies have been performed, assuming two values of the Reynolds number (*Re*), computed according to the maximum velocity in the ff region and the depth (y_{max} – H). The first study concerns the effect of the mesh refinement, without any special regard to the size and discretization of the TL. We set the size of the TL equal to y_{max}/1000. Results are summarized in tables 1,a-1,b of Fig. 2, in terms of L_2 norm of absolute and relative errors of the numerical solution compared to the analytical one in Eqs. (3). As expected, the convergence order is almost 1, due to the spatial approximation order of the velocity inside each triangle. The second study concerns the effect of the size of the TL, and the L_2 norms of the errors of the velocity have been reported in tables 2,a-2,b of Fig. 2. According to the definition of the velocity profile (in Eqs. (3)), function of the bulk value of the permeability k_0, we expect that the numerical solution converges to the exact one reducing the size of the TL. This is confirmed from the results in tables 2.

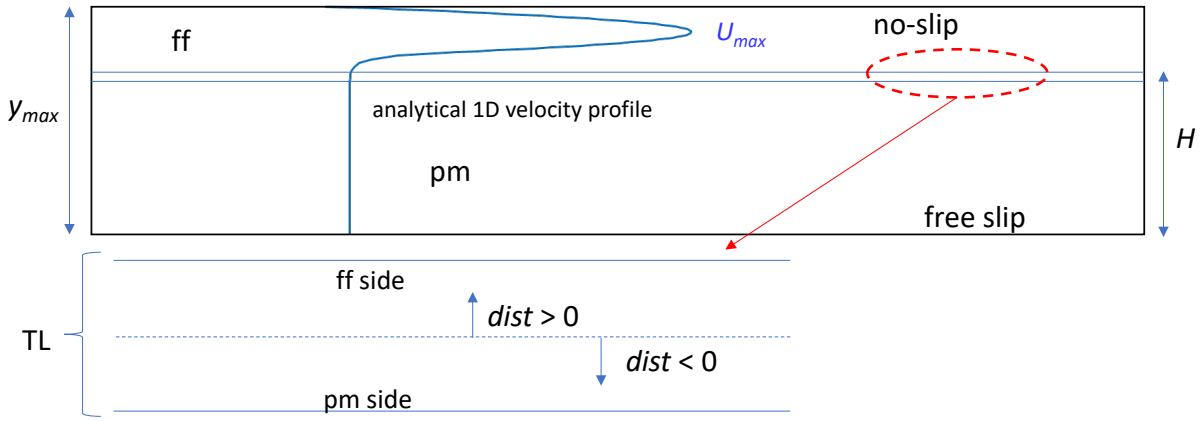

Figure 1. Test 1. Definition sketch

Materials Research Proceedings **26** (2023) 3-8 https://doi.org/10.21741/9781644902431-1

Effect of the size of the transition layer

Table 2,a Re 1.5

mesh linear size [m]	L2 ass err	L2 rel err	convergence	convergence
0.016	3.42E-05	1.57E+01		
0.008	1.71E-05	7.457924	1.00E+00	1.07E+00
0.004	8.26E-06	3.5568935	1.05E+00	1.07E+00
0.002	3.99E-06	1.70490455	1.05E+00	1.06E+00

TL size [m]	L2 ass err	L2 rel err	converger	converger
0.02	2.80E-05	8.863378		
0.005	1.30E-05	4.154056	1.11E+00	1.09E+00
0.00125	6.11E-06	2.022567	1.09E+00	1.04E+00
0.0003125	2.90E-06	0.9868	1.08E+00	1.04E+00

Table 2,b Re 150

mesh linear size [m]	L2 ass err	L2 rel err	convergence	convergence
0.016	3.61E-05	1.59E+01		
0.008	1.73E-05	7.90083	1.06E+00	1.01E+00
0.004	8.63E-06	3.789456	1.01E+00	1.06E+00
0.002	4.20E-06	1.833356788	1.04E+00	1.05E+00

TL size [m]	L2 ass err	L2 rel err	converger	converger
0.02	2.99E-05	9.054097		
0.005	1.40E-05	4.259854	1.09E+00	1.09E+00
0.00125	6.70E-06	2.129765	1.07E+00	1.00E+00
0.0003125	3.20E-06	1.030066	1.07E+00	1.05E+00

Figure 2. Test 1. Errors and study of the convergence order

2. Test 2. Free fluids over a porous obstacle. Isotropic and anisotropic cases

The geometry for this test is reported in Fig. 3. The working fluid is air. We set a pressure drop $\Psi_1 - \Psi_2$ = 1d-06 m^2/s^2. The permeability matrix **K** in the (bulk) porous medium is defined as

$$\mathbf{K} = \mathbf{RAR^{-1}} \qquad \mathbf{R} = \begin{pmatrix} \boldsymbol{cos\alpha} & \boldsymbol{-sin\alpha} \\ \boldsymbol{sin\alpha} & \boldsymbol{cos\alpha} \end{pmatrix} \qquad \mathbf{A} = \begin{pmatrix} k/\beta & \mathbf{0} \\ \mathbf{0} & k \end{pmatrix} \qquad (5),$$

with angle α defined in figure 3. The porosity in the porous medium is 0.4. We compare the results of the ODA solver with the DuMux TDA solver [8]. DuMux applies a monolithic approach, where the Navier-Stokes equations for the ff region and the Darcy equations for the pm are solved, along with the interface conditions (IFCs), are solved in one large system. The IFCs impose the equality of fluxes and momentum fluxes in the ff and pm regions along the normal direction to the interface, as well as the BJC for the velocity along the tangential direction to the interface.

For the ODA simulation, the mesh sizes range from 1d-05 m inside the TL to 2.5 d-02 m in the ff and pm bulk regions (see in figure 3 the zoom close to the TL region). For the DuMux simulation, a structured mesh is used to discretize the domain, with constant size 1d-04 m. We assumed a hyperbolic variation of porosity and permeability parameters, as in the previous test. We performed simulations assuming both isotropic and anisotropic porous obstacle.

For the isotropic case, we set α = 0 and k = 1d-08 m^2 in Eq. (5) and, for the ODA simulations, we assume two sizes of the TL, 1d-04 m and 5d-04 m. Due to the obstacle, a "channelized" flow is established above the porous medium, as shown in Fig. 4,a where we plot the flow field computed by the ODA solver. Similar overall results are given by the TDA solver (not shown for brevity). In Fig. 4,b-4,c, we compare, in the region close to the TL region, the velocity components along the vertical lines in the middle and at the upstream (left) side of the porous obstacle. Observe the differences, in the ODA solutions, due to the size of the TL, and the jump of the velocity component parallel to the interface in the DuMux results, due to the IFCs. Along the upstream side of the obstacle, the two solvers compute vertical velocity component v with opposite sign.

In the case of anisotropic obstacle, we set in Eq. (5) α = - π/4, k = 1d-06 m^2 and coefficient β = 100. The size of the TL for the ODA model is 5d-04 m. In Fig. 5,a we plot the velocity vectors computed by the ODA solver. Similar overall results are given by the TDA solver. In Fig. 5,b we show the differences of the velocity components along the vertical right boundary of the obstacle in the TL region. Observe the different sign of the u component. Interesting is the comparison of the pressure fields (in Fig. 5.c), The ODA solver computes local maxima and minima along the upstream and downstream sides of the obstacle, respectively, while DuMux computes almost constant pressure values upstream and downstream the porous medium.

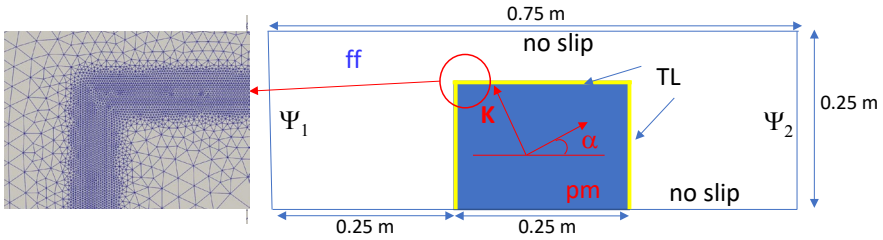

Figure 3. Test 2. Definition sketch. Boundary conditions, zoom of the mesh

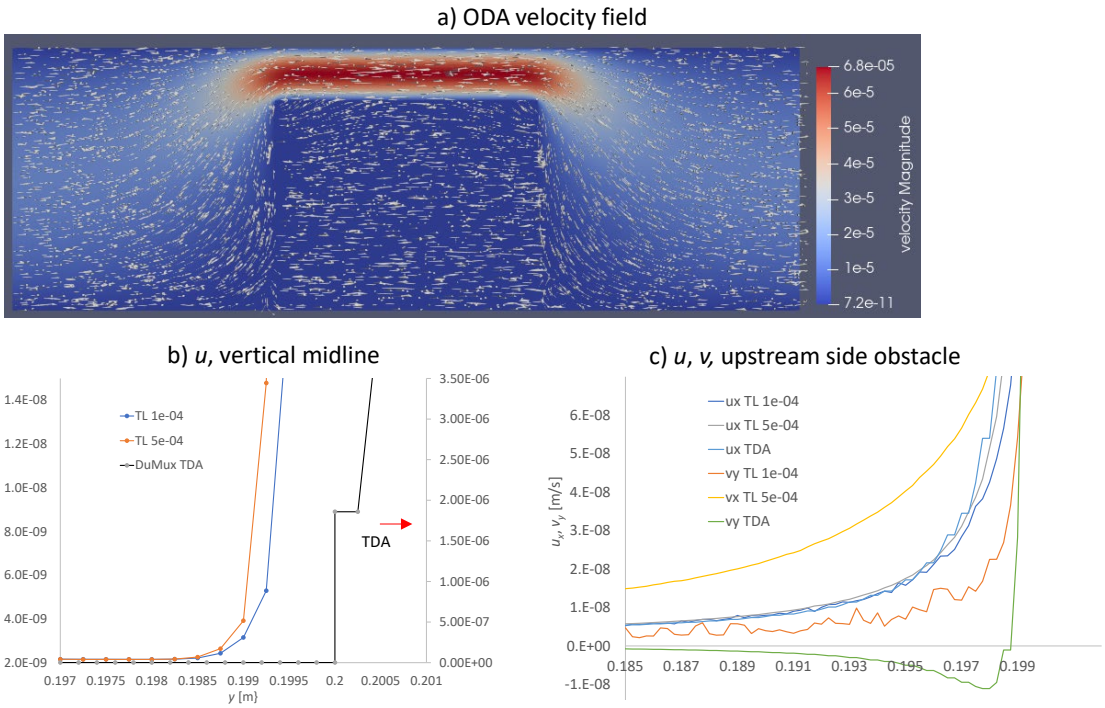

Figure 4. Test 2. Isotropic porous obstacle. a) velocity field, ODA solver. b) u component vertical midline of the obstacle. c) u and v components upstream side of the obstacle

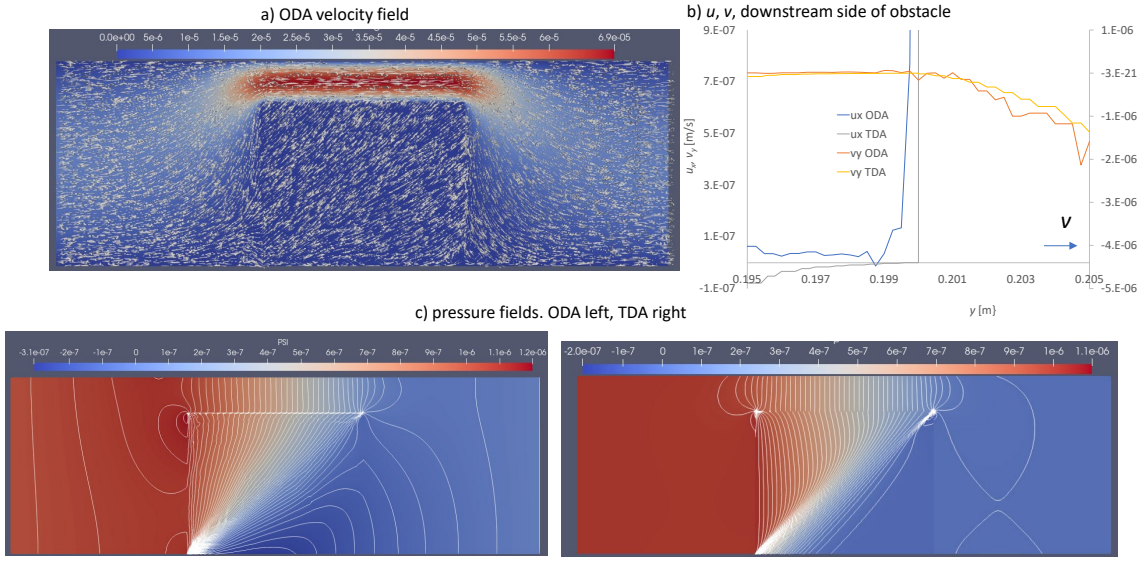

Figure 5. Test 2. Anisotropic porous obstacle. a) velocity field of ODA solver. b) u and v components at the downstream side of the obstacle, c) pressure fields, left ODA solver, right TDA solver

Conclusions

We have presented a new ODA numerical solver for the simulation of the interaction of free fluid over and inside a porous medium. This is a new research activity and we are aware that a lot of work have to be still done. According to the preliminary results shown in this paper, in-deep investigation deserves the role of the transition layer at the interface between the fluid and porous regions, along with its size and position. In the literature, there is a lack of studies regarding the comparison of the solutions provided by ODA and TDA models. Overall agreement has been obtained of the computed velocity fields far from the interfaces. Important differences of flow velocity and pressure fields have been obtained by the two approaches close to the transition layer. Prediction of transport phenomena of heat and species at interfaces could be strongly affected by the solutions of the velocity and pressure.

References

[1] B. Goyeau, D. Lhuillier, D. Gobina, M.G. Velarde, Momentum transport at a fluid–porous interface, Int. J. Heat and Mass Transfer 46 (2003) 4071–4081. https://doi.org/10.1016/S0017-9310(03)00241-2

[2] G.S. Beavers, D. D. Joseph, Boundary conditions at a naturally permeable wall, J. Fluid Mech. 30(01) (1967) 197–207. https://doi.org/10.1017/S0022112067001375

[3] L. Wang, L.-P. Wang, Z. Guo, J. Mi, Volume-averaged macroscopic equation for fluid flow in moving porous media, Int. J. Heat and Mass Transfer 82 (2015) 357–368. https://doi.org/10.1016/j.ijheatmasstransfer.2014.11.056

[4] H. Chen, X.-P. Wang, A one-domain approach for modeling and simulation of free fluid over a porous medium, J. Comp. Phys., 259 (2014) 650–671. https://doi.org/10.1016/j.jcp.2013.12.008

[5] F. J. Valdés-Parada, D. Lasseux, A novel one-domain approach for modeling flow in a fluid-porous system including inertia and slip effects, Phys. Fluids 33, 022106 (2021). https://doi.org/10.1063/5.0036812

[6] W. Gray, A derivation of the equations for multi-phase transport, Chemical Engineering Science Vol. 30, Issue 2, February 1975, Pages 229-233. https://doi.org/10.1016/0009-2509(75)80010-8

[7] C. Aricò, M. Sinagra, Z. Driss, T.Tucciarelli, A new solver for incompressible non-isothermal flows in natural and mixed convection over unstructured grids, Applied Mathematical Modelling 103 (2022), 445-474. https://doi.org/10.1016/j.apm.2021.10.042

[8] T. Koch, D. Gläser, K. Weishaupt, S. Ackermann, M. Beck, B. Becker, S. Burbulla, H. Class, E. Coltman, S. Emmert, T. Fetzer, C. Grüninger, K. Heck, J. Hommel, T. Kurz, M. Lipp, F. Mohammadi, S. Scherrer, M. Schneider, G. Seitz, L. Stadler, M. Utz, F. Weinhardt, B. Flemisch, DuMux 3 – an open-source simulator for solving flow and transport problems in porous media with a focus on model coupling, Comp. Math. with Applications 81 (2021) 423–443. https://doi.org/10.1016/j.camwa.2020.02.012